Aperiodic and modulated Pb thin films on fivefold icosahedral Al-Cu-Fe and Al(111): Tailoring the structure of Pb

Th. Deniozou, J. Ledieu, and V. Fournée
Institut Jean Lamour, UMR 7198 CNRS - Nancy Université - UPV Metz, Ecole des Mines de Nancy, Parc de Saurupt, CS 14234, 54042 Nancy Cedex, France

D. M. Wu and T. A. Lograsso
Ames Laboratory, Iowa State University, Ames, Iowa 50011, USA

H. I. Li and R. D. Diehl
Department of Physics, Pennsylvania State University, University Park, Pennsylvania 16802, USA
(Received 16 February 2009; published 5 June 2009)

We report on the growth of Pb thin films deposited either on the Al-rich fivefold surface of the icosahedral Al-Cu-Fe quasicrystal or on the (111) surface of fcc Al. On the quasicrystalline substrate, the diffusion length of Pb adatoms is short due to heterogeneous nucleation that enforces a quasiperiodic structure in the monolayer. On the Al(111) substrate, the mobility of Pb adatoms is high and the interaction with the substrate is flatter, leading to the formation of a $(\sqrt{31}\times\sqrt{31})R8.95°$ higher-order commensurate structure. This moiré structure propagates up to the highest coverages investigated.

DOI: 10.1103/PhysRevB.79.245405 PACS number(s): 68.37.Ef, 68.35.Rh, 71.23.Ft, 71.15.Mb

I. INTRODUCTION

Using epitaxy, it is possible to change the nature of simple metals by forcing thin films to adopt a structure different from its bulk form. In this spirit, growth of metal layers on quasiperiodic surfaces has attracted considerable interest in recent years, driven by the expectation that the aperiodicity of the substrate can propagate in the film.[1–3] Quasicrystals are complex intermetallics exhibiting long-range aperiodic order and noncrystallographic rotational symmetry (usually fivefold or tenfold symmetry). First discovered by Shechtman *et al.*,[4] they are found as stable phases in several binary or ternary systems.[5] The physical properties associated with quasiperiodic structures significantly depart from those of periodic alloys.[6] One of the most surprising features is probably the nonmetallic behavior of the electrical conductivity in Al-based quasicrystals. Thus, the question arises whether a single element deposited onto a quasicrystalline surface can adopt a quasiperiodic structure and what are the resulting properties of such a new material.

A number of experiments have been performed to answer these questions. In some cases, metal adatoms adopt the substrate structure only at a very local scale. For example, Al adatoms nucleate into fivefold symmetric islands on the fivefold surface of the icosahedral (*i*-) Al-Cu-Fe quasicrystal.[7] In other cases, a quasiperiodic modulation in the film structure is observed which persist through several crystalline overlayers. Examples are Cu or Co thin films deposited on the fivefold surface of the *i*-Al-Pd-Mn quasicrystal or the tenfold surface of the decagonal (*d*-) Al-Ni-Co quasicrystal.[8–10] A true two-dimensional (2D) quasiperiodic structure has been achieved only for specific elements, typically low melting point elements such as Pb, Bi, Sb, and Sn or rare gases such as Xe.[11–15]

First, Franke *et al.*[11] reported evidence for the formation of quasiperiodic Bi or Sb monolayers (MLs) deposited on either the fivefold surface of the *i*-Al-Pd-Mn or the tenfold surface of the *d*-Al-Ni-Co. The quasiperiodic structure of the monolayers was characterized using low-energy electron diffraction (LEED) and helium atom scattering. Later studies demonstrated the structure of the first quasiperiodic Bi wetting layer using scanning tunneling microscopy (STM).[16–18] Similar observations were made for Sn deposited on the fivefold surface of the *i*-Al-Cu-Fe quasicrystal.[14] A structure model for the Bi monolayer was proposed by Krajci and Hafner[19] based on *ab initio* density-functional calculations. The importance of the adsorbate-substrate interaction was emphasized in order to stabilize the quasiperiodic layer. In particular, the potential-energy surface seen by an adatom shows strong minima at the vertices of the quasiperiodic tiling used to describe the substrate structure, thus enforcing the quasiperiodic structure of the film. From these studies, it appears that only the first monolayer can adopt the quasiperiodic structure. Once it has been completed, a structural transition toward a crystalline structure usually occurs. This transition has been investigated, for example, for the case of Xe layers physisorbed on the tenfold surface of *d*-Al-Ni-Co.[15,20] Both LEED experiments and grand canonical Monte Carlo simulations demonstrated that the film is epitaxial in the first layer but evolves into a bulklike sixfold structure in the second layer. A molecular-dynamics study of the structure of adlayers on a quasicrystalline substrate pointed out the importance of the adatom-adatom interactions with respect to the adatom-substrate interaction.[21] Stronger adatom-substrate interactions (and lower adsorption temperature) promote pseudomorphic 2D growth.

Recently, we have reported the formation of a quasiperiodic Pb monolayer on the fivefold surface of the *i*-Al-Pd-Mn.[12] *In situ* STM experiments clearly show how the quasiperiodic structure of the substrate propagates into the film. The growth proceeds via self-assembly of an interconnected network of small Pb islands with pentagonal

shape. These fivefold clusters are monoatomic in height and have an apparent edge length equal to 4.9 ± 0.3 Å, i.e., τ bigger than the smallest Al pentagonal motifs present on the clean surface [with $\tau=(1+\sqrt{5})/2=1.618\ldots$ the golden mean]. The completion of the monolayer is achieved by filling the interstices of the interconnected network of pentagonal Pb islands. The quasiperiodic monolayer can be formed within a broad range of temperature from 57 to 653 K. Its structural quality is improved by annealing. The density of the Pb monolayer (0.09 atom/Å^2) has been deduced from x-ray core-level photoemission. This value is very similar to the density of Al atoms in the topmost layer of the substrate. This quasiperiodic Pb monolayer exhibits properties which are fundamentally different from those of bulk Pb. The most striking evidence is the wide pseudogap in the electronic density of states at the Fermi level observed by scanning tunneling spectroscopy and ultraviolet photoemission spectroscopy.

Surprisingly, once the wetting layer has been completed, the growth of a second layer is not observed, at least within the range of fluxes used ($2.5\times10^{-3}-2.5\times10^{-2}$ ML s^{-1}). This is also observed for low-temperature deposition (57 K). It suggests that the sticking coefficient of Pb on a quasiperiodic Pb surface is close to zero, which is unusual for metal adsorption on metal surfaces. An alternative explanation could be that Pb adatoms become extremely mobile on the first Pb monolayer and form very large isolated clusters covering a very small fraction of the surface area and thus hardly detectable by surface science technique.

Here we report on the growth of Pb thin films on the fivefold surface of the *i*-Al-Cu-Fe and on the Al(111) surface. The quasicrystalline *i*-Al-Cu-Fe and *i*-Al-Pd-Mn phases are isostructural and the structure of the fivefold surface of the *i*-Al-Cu-Fe has been described in the light of a refined structure model.[22–24] It has been found that the surface corresponds to a bulk truncation with no reconstruction or chemical segregation. The surface is formed at dense Al-rich layers separated by large interlayer spacings. Therefore, it is important to compare the growth of Pb thin films on the Al-rich planes exposed by the fivefold *i*-Al-Cu-Fe surface with Pb deposition on Al(111). We will see that although the chemistry of both surfaces is comparable, the growth modes are drastically different. Experimental details are provided in Sec. II. In Sec. III we first describe the growth of a Pb thin film on the fivefold *i*-Al-Cu-Fe surface. Then, we describe the growth of Pb on Al(111) for coverages ranging from 0.5 to 30 ML. The two different growth modes are compared and discussed in Sec. IV and we provide a short summary.

II. EXPERIMENTAL DETAILS

A clean fivefold surface of the *i*-$Al_{63}Cu_{24}Fe_{13}$ was prepared by repeated cycles of sputtering (Ar^+, 2 keV) and annealing (913 K). The quasiperiodic structure of the surface was checked by LEED and STM. Lead was deposited at room temperature using an Omicron e-beam heated evaporator. The pressure during deposition was kept in the low 10^{-10} mbar range. The Al(111) substrate was prepared by sputtering (Ar^+, 2 keV, 15 min) and annealing up to 773 K.

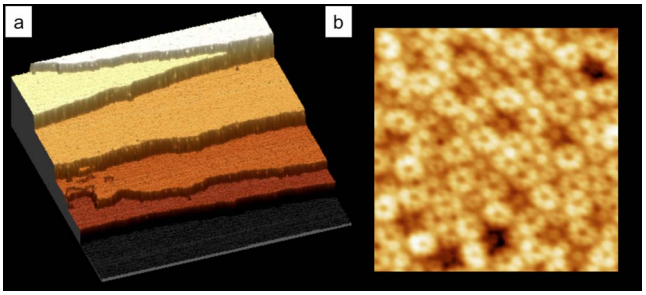

FIG. 1. (Color online) (a) STM images of the fivefold *i*-Al-Cu-Fe surface showing a terrace and step morphology (500×500 nm^2) and (b) typical fivefold symmetric local configurations (18×18 nm^2).

The growth of a Pb thin film on the Al(111) substrate was monitored from submonolayer coverage up to 30 ML by LEED and STM. The deposition flux was calibrated by directly measuring the coverage in STM images. Further characterization was carried out by x-ray photoelectron spectroscopy (XPS) using an Mg Kα anode (1253.6 eV).

III. RESULTS

A. Pb adsorption on the fivefold surface of the *i*-Al-Cu-Fe quasicrystal

The structure of the fivefold surface of *i*-Al-Cu-Fe has been described previously.[24] Here we recall the main characteristics. Figure 1 shows the terrace and step surface morphology resulting from the sputter-annealing treatment. There are two basic step heights $S=0.4$ nm and $L=\tau\cdot S$, where τ is the golden ratio 1.618…. Larger step heights h are also observed, which can be expressed as linear combinations $h=mS+nL$ with (m,n) integers. The S and L step heights correspond to the thickness of blocks of layers separated by gaps, which are stacked along the fivefold axis according to a Fibonacci sequence.[24] As seen in Fig. 1(a), a terrace width of about 100 nm is typical. The rms roughness measured on individual terraces is about 0.02 nm. On such flat terraces, it is possible to obtain high-resolution STM images [Fig. 1(b)] which can be interpreted using the bulk structure model. Typical motifs of icosahedral surfaces are the so-called *dark stars* and *white flowers*.[25] The same motifs can be recognized in dense Al-rich planes of the bulk model separated from adjacent planes by large gaps. A section of one such bulk plane is shown in Fig. 2. The smallest motifs are Al pentagons with edge length of 2.99 Å. They are frequently incomplete. Five such pentagons decorating a larger pentagon of edge length 4.8 Å (i.e., τ scaled compared to Al pentagons) constitute the backbone of the dark stars (Fig. 2). The white flower feature is also shown in Fig. 2. One central atom is surrounded by a decagonal ring of radius equal to 9.4 Å decorated by five Al pentagons. The centers of these five Al pentagons define a larger pentagon of edge length 7.8 Å (i.e., τ^2 scaled compared to Al pentagons). The white flowers themselves decorate larger pentagonal motifs as seen in Fig. 2 with an edge length of about 20 Å. Several bulk structure models have been proposed for this class of quasi-

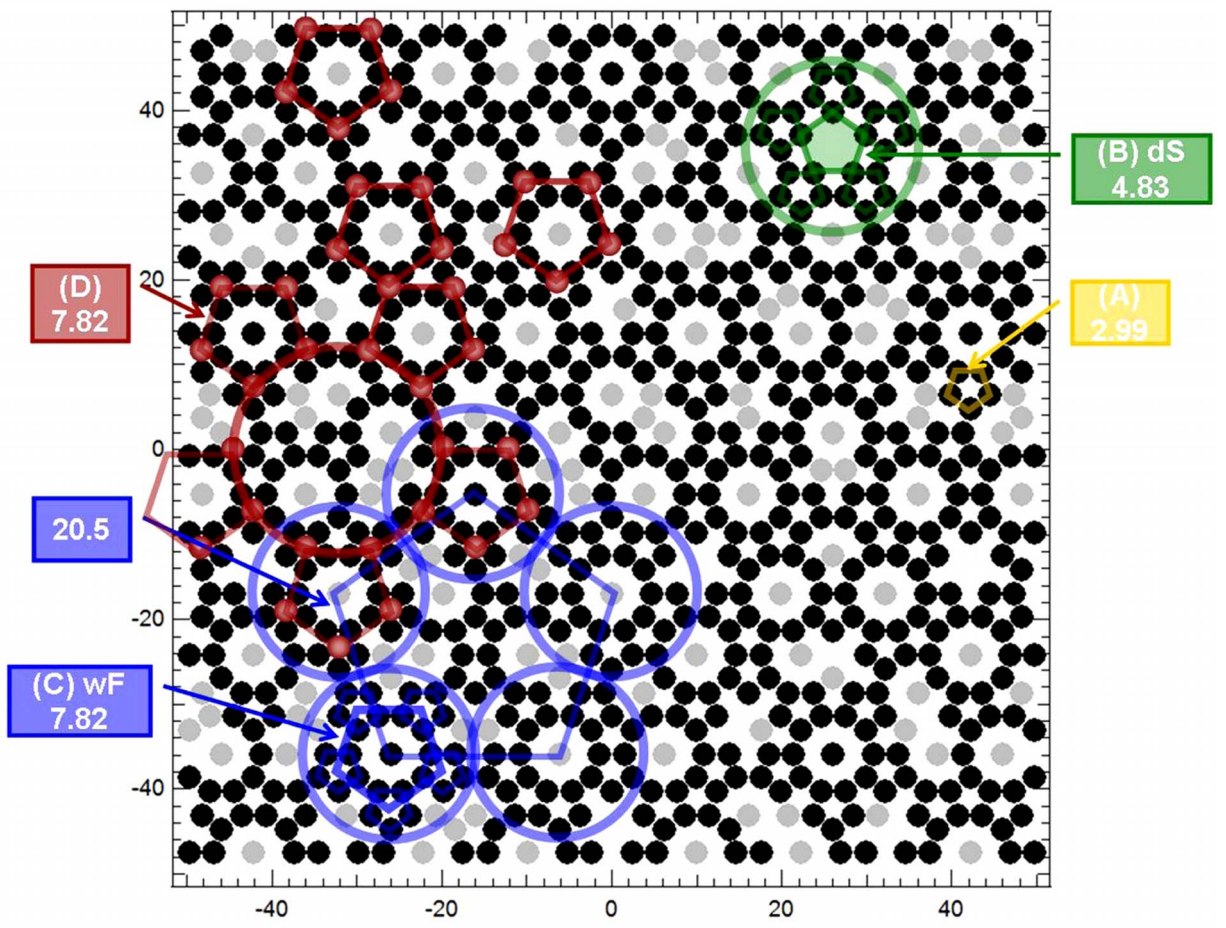

FIG. 2. (Color online) Atomic positions in a plane (10×10 nm^2) generated from experimental bulk structure model. Black circles: Al atoms. Gray circles: Fe atoms. The smallest Al pentagonal motif [(A): yellow], the dark stars (dS) [(B): green], and the flowerlike (wF) features [(C): blue] are highlighted on the figure. Possible adsorption sites for Pb atoms [(D): red] have been added to the model, together with the edge lengths of the various resulting pentagonal motifs.

crystalline phases and the chemistry of the top surface planes slightly varies from model to model.[26] Nevertheless, there are strong indications that the top surface planes contain 85%–100% of Al. We use this surface as a template to grow Pb thin films.

Figure 3 shows STM images of the surface for a coverage of 0.4 ML. Lead adatoms are identified as bright dots in the STM images. They are mainly isolated features rather than embedded in compact islands, suggesting a rather short diffusion distance on the quasiperiodic substrate. However, the positions of Pb adatoms are not random and pentagonal features can be recognized. In addition, the fast Fourier transform (FFT) of the image still exhibits a tenfold pattern consistent with the expected fivefold symmetry for pseudomorphic growth. The smallest Pb pentagons have an edge length of 8.0 ± 0.3 Å. This value is close to the edge length of the pentagons defined by the five petals of the flowerlike motifs. We note that Al pentagons forming the flowers have been identified as either truncated or hanging Bergman clusters.[25,26] These two types of clusters are the building blocks of this family of quasicrystals and any surface necessarily cuts some of these clusters.[26,27] Several studies have identified these cut clusters as strong adsorption sites.[7,28–32] Therefore the 8.0 Å Pb pentagons might result from the preferential adsorption of adatoms at these specific sites. The motif shown in Fig. 3(b) consists of one central atom surrounded by a decagonal ring of radius equal to 25 ± 1 Å and surrounded by five incomplete 8 Å Pb pentagons. This geometrical motif formed by Pb adatoms corresponds to the

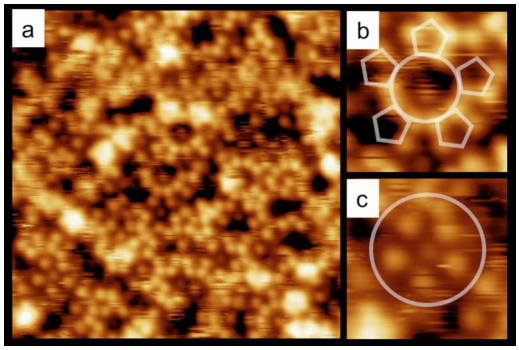

FIG. 3. (Color online) (a) STM images of Pb film on the fivefold surface of *i*-Al-Cu-Fe surface for an estimated coverage of 0.4 ML (25×25 nm^2). [(b) and (c)] High-resolution image showing typical fivefold symmetric configurations (6×6 nm^2).

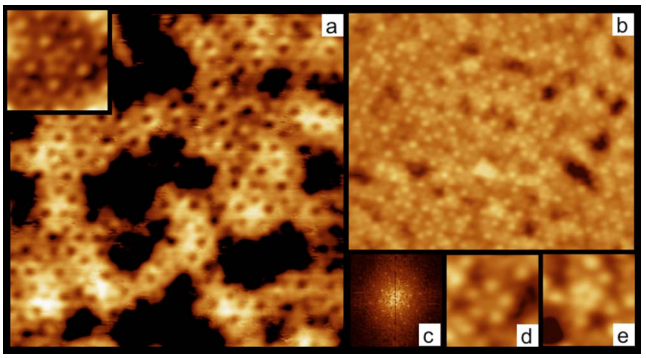

FIG. 4. (Color online) STM images of the Pb film on the fivefold surface of *i*-Al-Cu-Fe surface. In (a), the estimated coverage is 0.7 ML (26×26 nm^2 and the inset is 7×7 nm^2). In (b)–(e), the monolayer has been completed [(b): 25×20 nm^2, (c) the corresponding FFT, and (d) and (e) show typical fivefold symmetric configurations (4×4 nm^2)].

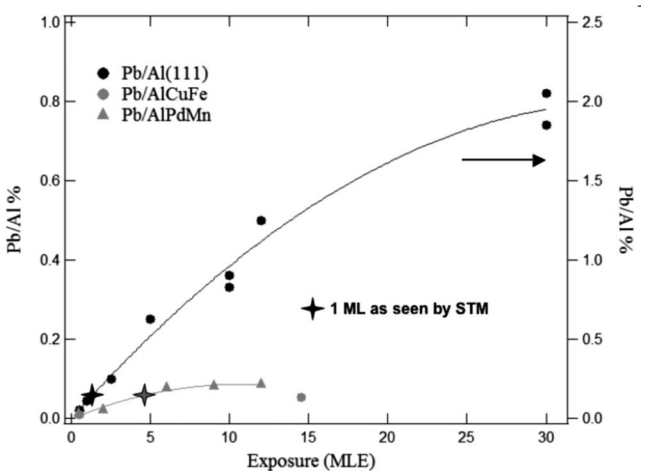

FIG. 5. Intensity ratio between the Pb $4f$ and Al $2s$ XPS core levels measured as a function of exposure in units of monolayer equivalent for different systems. The cross symbols indicate completion of the monolayer as seen by STM.

flowerlike motif of the clean surface but τ^2 scaled. Other typical geometrical features are dark stars pointing up in the STM images [see Fig. 3(c)] arising from the contrast produced by five Pb adatoms forming a pentagon of edge length equal to 14 Å and pointing downward. These dark stars are similar to the dark star features observed on the clean surface but again scaled by a factor τ^2 and decorated in its center.

With increasing deposition time, the Pb film becomes denser and appears as a network of pentagonal features at 0.7 ML [Fig. 4(a)]. Figure 4(b) corresponds to a full monolayer deposited at room temperature and shows a well-ordered structure. The FFT of this image is shown in Fig. 4(c) and exhibits three rings of ten diffraction spots whose diameters scale like $1:\tau:\tau^2$. This indicates that the Pb monolayer has a quasiperiodic structure. The smallest pentagonal motifs observed on the complete monolayer are shown in Figs. 4(d) and 4(e) and have edge lengths of 4.8, 8, and 14 Å.

These results are consistent with our previous observations that Pb films deposited on either the fivefold surface of the *i*-Al-Pd-Mn or the tenfold surface of the *d*-Al-Ni-Co adopt a quasiperiodic structure.[12,13] The size of the smallest pentagonal Pb feature observed in this study (edge length ~4.8 Å) is similar to what was observed on *i*-Al-Pd-Mn substrate (~4.9 Å). The smallest pentagonal structural elements present on the clean substrate have an edge length of 3.0 Å, i.e., smaller than the smallest pentagon within the Pb structure. This scaling of the basic structural elements is consistent with the scaling of the complete monolayer structure reported previously. However, there is a difference in the way the growth proceeds on these two substrates. On the fivefold surface of the *i*-Al-Pd-Mn, a network of pentagonal islands (4.9 Å edge length) develops in the early stage of the growth (0.2 ML). On the fivefold surface of the *i*-Al-Cu-Fe substrate, the mobility of Pb adatoms seems to be reduced and the formation of islands is not obvious from STM images at low coverage. Instead, Pb adatoms appear to decorate the quasiperiodic lattice by adsorption at specific sites.[26] Then, the Pb film becomes denser upon further deposition and a compact network of pentagonal features is observed only at 0.7 ML. Once the monolayer has been completed, the structure of the Pb films formed on these two substrates appears comparable. It is worth mentioning that no chemical shift could be observed in Pb core-level binding energies recorded by XPS either on Pb monolayers on quasicrystalline substrates or on thick Pb films deposited on Al(111). In addition, Pb and Al are immiscible in the bulk. Both observations further support the absence of intermixing or surface alloying in this system.

Another similarity between both icosahedral substrates is the observation that the sticking coefficient of Pb decreases to zero upon completion of the first monolayer, at least for deposition fluxes in the range of 10^{-3}–10^{-2} ML s^{-1}. As a result, quasicrystalline substrates must be exposed to 4–5 monolayer equivalents (MLEs) in order to complete the monolayer. This is shown in Fig. 5 where the intensity ratio between Pb $4f$ and Al $2s$ core levels has been plotted as a function of the exposure in MLE units for the fivefold *i*-Al-Cu-Fe and *i*-Al-Pd-Mn substrates. Once the monolayer has been completed as seen by STM, the intensity ratio saturates meaning that Pb does not stick on the quasiperiodic Pb first layer. This puzzling behavior has not received any explanation yet. For comparison, Fig. 5 also shows the intensity ratio measured for Pb thin films on Al(111). The intensity ratio ($I_{\mathrm{Pb}}/I_{\mathrm{Al}}$) measured on quasicrystalline substrates has been scaled such that the ratio ($I_{\mathrm{Pb}}/I_{\mathrm{Al}}$) measured for the complete monolayer match ($I_{\mathrm{Pb}}/I_{\mathrm{Al}}$) measured for 1 ML deposited on Al(111) as seen by STM. The ratio ($I_{\mathrm{Pb}}/I_{\mathrm{Al}}$) continuously increases for Pb on Al(111) and saturates at the highest coverages because Al cannot be detected by XPS when the thickness of the Pb film becomes large compared to the photoelectron escape depth. An alternative explanation could be that Pb adatoms become extremely mobile on the first Pb monolayer and form very large isolated clusters. In this case, these Pb mounds would cover only a very small fraction of the surface area and would not contribute significantly to the photoemitted intensity. Such behavior has already been observed for Pb deposited on various semiconductor surfaces at room temperature.[33]

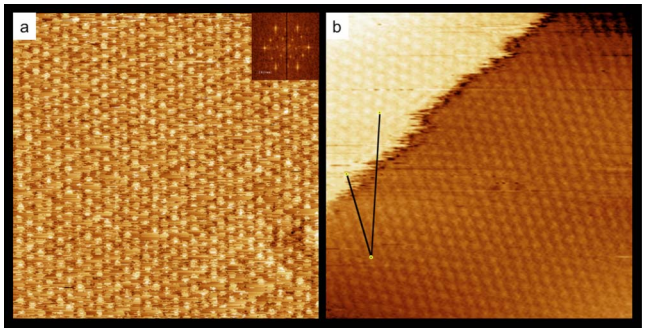

FIG. 6. (Color online) STM image of Pb overlayer on Al(111) showing either the Pb lattice as in (a) (1 ML, 10×10 nm^2, inset is the Fourier transform) or (b) the 8 Å moiré lattice (10 ML, 20 $\times20$ nm^2). The rotation between two moiré lattices observed on adjacent terraces is 19°.

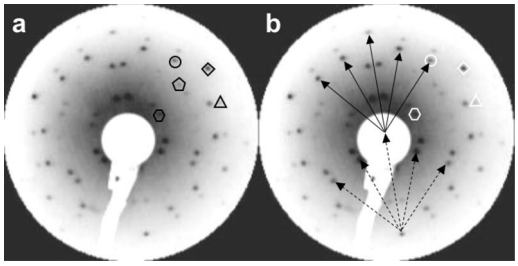

FIG. 7. (a) LEED pattern for one monolayer of Pb on Al(111) at $E=70$ eV. The spots indicated by signs correspond to those described in Table I. A first-order substrate spot is indicated by the diamond shape. (b) The same LEED pattern as in (a), indicating reciprocal-lattice vectors for single scattering from the substrate or overlayer (top arrows) and double scattering by the substrate and the overlayer (bottom arrows).

B. Pb adsorption on the Al(111) surface

To compare further these systems, we report below the growth of Pb thin films on Al(111) investigated by STM and LEED. Both Pb and Al elements crystallize into the face-centered-cubic lattice but the lattice mismatch is rather large $[(a_{\mathrm{Pb}}=4.95\ \text{Å}/a_{\mathrm{Al}}=4.05\ \text{Å})=1.22]$. To the best of our knowledge, the growth of Pb thin films on Al(111) system has not been reported yet. Related studies include an analysis of the solidification of Pb particles embedded in an Al matrix and their orientation relationships. Experiments suggest that Pb precipitates in the cubic matrix with a cube-on-cube orientation relationship.[34] The Pb/Al interface has also been investigated in a recent computer simulation.[35] An epitaxial relationship was predicted with no rotation between the two lattices. In addition, the formation of a moiré superstructure was mentioned due to the 22% lattice mismatch. Moiré patterns are frequently observed for incommensurate systems, not only in metal-on-metal systems but for other systems as well.[36–38] A general property of such superstructures is that the lateral interaction within the film must be large compared to substrate-film lateral interaction in order to be formed. Experimentally, a hexagonal moiré pattern has been observed by STM (Ref. 37) and LEED (Ref. 39) in a Pb monolayer deposited on Ag(111). This system must be closely related to Pb on Al(111) as the lattice parameters of Ag and Al differ by less than 1%. It was found that two equivalent Pb domains coexist, rotated by $\pm4.5°$ with respect to the Ag lattice. The hexagonal unit cell of the moiré modulation is denoted by $(\sqrt{28}\times\sqrt{28})R19.1°$ with respect to the Ag substrate and $(\sqrt{19}\times\sqrt{19})R23.4°$ with respect to the Pb lattice. A similar superstructure can be expected for Pb on Al(111) depending on the relative strength of the lateral interaction with respect to the lateral interactions with the Al substrate.

Figure 6 shows STM images of the Al(111) surface exposed to 1 and 10 MLE of Pb. It is observed that the Pb film grows in a perfect layer-by-layer mode. This is consistent with the low surface energy of Pb compared to that of Al ($\gamma_{\mathrm{Pb}(111)}=0.312\ \mathrm{J\ m^{-2}}$ and $\gamma_{\mathrm{Al}(111)}=1.199\ \mathrm{J\ m^{-2}}$) (Ref. 40) that drives a Frank–van der Merwe growth mode. At low coverage, STM images show that Pb islands nucleate at step edges. Isolated Pb islands on Al terraces were not observed for room-temperature deposition, up to the highest coverages investigated in the present study (30 MLE), suggesting that the diffusion length of Pb adatoms is large compared to the average terrace width (~70 nm). The steps appear fuzzy [Fig. 6(b)], a feature usually ascribed to high atom mobility along step edges. For film thicknesses corresponding to an integer number of monolayers, a step height value of 2.35 ± 0.1 Å is deduced from height histogram calculated from STM images spanning adjacent terraces. This value is in agreement with the interplanar distance separating (111) substrate planes ($a_{\mathrm{Al}}/\sqrt{3}=2.33$ Å). For intermediate coverages, additional step heights of 2.80 ± 0.1 Å are also measured, corresponding to the Pb(111) interplanar spacing ($a_{\mathrm{Pb}}/\sqrt{3}=2.85$ Å) as well as smaller step heights of 0.5 ± 0.1 Å. The latter ones correspond to the height difference between Pb and Al (111) slabs. High-resolution STM images of the Pb films have been obtained for coverages ranging from 1 to 10 ML. Different structures are observed for all film thicknesses depending on the tip bias and conditions. The most frequently observed structure is a moiré lattice with parameter equal to 8.0 ± 0.2 Å. This superstructure exists according to two different orientations. This is illustrated in Fig. 6(b), where the moiré is easily recognized on two adjacent terraces but rotated by 19° from each other. For different tunneling or tip conditions, the Pb hexagonal lattice is observed with parameter equal to 3.5 ± 0.1 Å [Fig. 6(a)], in agreement with the nearest-neighbor distance of Pb (3.5 Å). Again, the Pb lattice is observed according to two different orientations rotated from each other by 19° on adjacent terraces.

Figure 7(a) shows the LEED pattern from a monolayer of Pb on Al(111) at 70 eV. Spots that are representative of four different 12-spot groups are indicated by different symbols and their momentum transfers are listed in Table I along with their corresponding real-space distances and their epitaxial angles relative to the Al(111) lattice. These parameters were measured relative to the Al(111) lattice spots, which was taken to have the bulk Al-Al spacing of 2.86 Å.

This LEED pattern can be completely explained in terms of an overlayer having a rotated lattice with a unit-cell length of 3.48 Å and an orientation of $\pm19°$ relative to the substrate lattice, and with additional diffraction spots arising

TABLE I. Measured parameters from the LEED pattern shown in Fig. 7. The real-space distance is the distance corresponding to a hexagonal unit-cell length, derived from the measured spot spacings, referenced to the Al-Al spacing of 2.86 Å.

Sign	Real-space distance (Å)	Epitaxial angle (deg)
Diamond	2.86	0
Hexagon	8.18 ± 0.07	9 ± 1
Pentagon	4.15 ± 0.06	5 ± 1
Circle	3.48 ± 0.03	19 ± 1
Triangle	3.05 ± 0.04	20 ± 1

from multiple diffraction from the substrate and overlayer. In Fig. 7(b), a first-order substrate reciprocal-lattice vector is shown along with four reciprocal-lattice vectors corresponding to first-order overlayer spots (plain arrows). The additional diffraction spots in this pattern can be obtained by summing substrate and overlayer reciprocal-lattice vectors. The dotted vectors show the same overlayer vectors added to a first-order substrate vector. Thus, all of the indicated spots and those that are equivalent by rotational symmetry arise from either single scattering from either the substrate or the overlayer, or by double scattering by a reciprocal-lattice vector of each. The spot indicated by triangles in Fig. 7(a) and its rotational equivalents can be generated by a triple-scattering event involving two first-order substrate vectors and one overlayer vector.

One way to verify the contribution of multiple scattering to these spots is to compare the energy dependence of their intensities to those of the substrate spots. Since for a monolayer structure, the substrate generally is a stronger scatterer (having contributions from more atoms), the intensity of the multiple diffraction spots track with the intensities of the substrate spots related to their scattering. We have checked the energy dependence of double diffraction spots arising from electrons that scatter by a substrate wave vector plus one of the overlayer wave vectors. The intensities of the double diffraction spots track the intensity of the substrate spots, which indicates that multiple diffraction is the dominant contributor to these diffraction spots.

This multiple diffraction explanation for the LEED pattern is a simple and valid way to account for all of the observed diffraction spots but the STM images from this film (Fig. 6) suggest that some diffraction intensity at the multiple diffraction locations may be due to satellite peaks that arise from a modulation of the overlayer structure. In the STM images, the dominant modulation period is about 8 Å, rotated by about 10° relative to the Al lattice. The simplest interpretation of this modulation is that it is a moiré pattern resulting from the interference of the different lattice spacings of the Al(111) surface and the Pb film. The fact that it is periodic suggests that the Pb structure is a higher-order commensurate structure (HOC), i.e., the film structure is periodic but not primitive with Pb atoms occupying different sites within the HOC unit cell. The different environments of the Pb atoms, along with any relaxation of their locations from a perfect triangular lattice, will contribute to the moiré interference pattern.

In order to determine this HOC structure, we have employed a systematic approach called the "hexagonal number sequence" method proposed by Tkatchenko,[41] as follows. The method as described here applies to hexagonal overlayers on hexagonal substrates.

The lattice vectors for the Al(111) substrate surface can be represented by $\mathbf{a_1}=(1,0)a$ and $\mathbf{a_2}=(1/2,\sqrt{3}/2)a$, where $a=2.86$ Å is the nearest-neighbor distance of the Al atoms. Any lattice point of the substrate can be described as a linear combination of these primitive vectors, $R=m\mathbf{a_1}+n\mathbf{a_2}$, where m and n are integers. For any commensurate or HOC layer on this substrate, the lattice vectors of the overlayer can be described by the lattice vectors

$$\mathbf{A_1}=\mathbf{R_0} \text{ and } \mathbf{A_2}=\begin{pmatrix} \frac{1}{2} & -\frac{\sqrt{3}}{2} \\ \frac{\sqrt{3}}{2} & \frac{1}{2} \end{pmatrix}\mathbf{R_0},$$

where $R_0=m_0\mathbf{a_1}+n_0\mathbf{a_2}$, where m_0 and n_0 are integers. The total number of atoms (or molecules) in either the substrate or the overlayer can be expressed with the same mathematical form, $N=m^2+n^2+mn$ or $N_0=m_0^2+n_0^2+m_0n_0$ for the substrate and adsorbate, respectively. Each combination of m, n, m_0, and n_0 represents a different commensurate structure of the system and possesses a different relative-lattice constant and a different rotation angle. By listing all possible m, n, m_0, and n_0 combinations, it is possible to identify which structures have the measured characteristics.

With no other constraints, this method will produce an infinite number of HOCs that will fit the experimentally measured parameters because any combination of parameters can be generated using a large enough HOC unit cell. In reality, the size of the HOC unit cell is limited in an experiment by the perfection of the crystal. In this experiment, we are able to utilize an additional constraint on the HOC unit-cell size from the moiré patterns in the STM image. Considering all possible HOC structures having a period of less than about 40 Å, we find that the best match with the measured parameters has the unit cell $(\sqrt{31}\times\sqrt{31})R8.95°$, shown in Fig. 8.

In this HOC structure, there are three fundamental periods: 2.86 Å from the Al lattice, 3.5 Å from the Pb lattice, and 15.9 Å from the moiré lattice. The angle between the Al and Pb primitive unit cells is 19.84°, compared to $19 \pm 1°$ measured from the LEED patterns. The angle between the Al unit cell and the HOC unit cell is 8.95°, compared to the 9° angle between the substrate and 8 Å spots in the LEED pattern. However, this HOC unit cell has a length of 15.9 Å rather than 8 Å. Inspection of Fig. 8 indicates that there is no periodic structure near 8 Å for the correct angles. However, if we consider a hard-sphere model for this HOC structure and look at the height profile of the atoms, we find that this structure does possess a 8 Å period height modulation.

Figure 9(a) shows a schematic diagram of the structure depicted in Fig. 8 but using partially transparent circles to denote atoms. In such a diagram, the darkness is related to the height of the overlayer Pb atoms. The height resolution is poor in such a diagram, i.e., there are only three possible heights but it turns out to be useful for illustrating the spatial

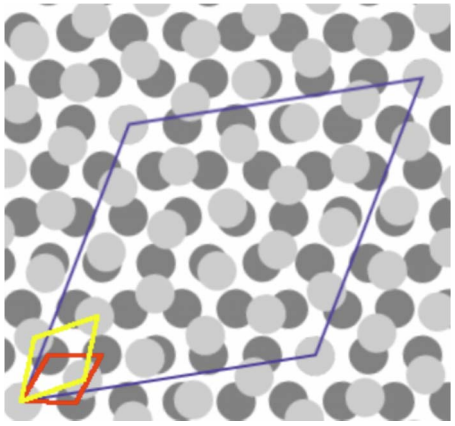

FIG. 8. (Color online) Schematic diagram of the ($\sqrt{31} \times \sqrt{31}$)$R8.95°$ HOC structure with dark circles representing the locations of Al atoms and light circles representing the locations of Pb atoms. The Al substrate unit cell having a length of 2.86 Å is shown by the red rhombus, the Pb overlayer unit cell having a length of 3.5 Å is shown by the yellow rhombus, and the HOC unit cell is shown by the blue rhombus of length $\sqrt{31} \times 2.86 = 15.9$ Å.

variations that produce the periods observed in the STM images. In Fig. 9(b), the plot in Fig. 9(a) is converted into a three-dimensional (3D) diagram, where the height (proportional to darkness) is plotted as a function of x-y position and then smoothed. The smoothed diagram has a clear "period" that is half of the unit cell, which corresponds well to the STM observations [see Fig. 6(b)]. Note that the degree of smoothing effectively degrades the lateral resolution of the structure, making it comparable to the STM image.

IV. DISCUSSION AND SUMMARY

We have shown that Pb deposited on the fivefold surface of the *i*-Al-Cu-Fe quasicrystal form a pseudomorphic monolayer. From the size of the pentagonal motifs identified in high-resolution STM images, it appears that the apparent structure of the monolayer as seen by STM is τ inflated compared to the bare substrate. These results are consistent with previous observations reported for Pb monolayers formed on the isostructural *i*-Al-Pd-Mn quasicrystal. However differences exist between the two systems in the low-coverage regime. In the case of the *i*-Al-Pd-Mn substrate, Pb adatoms are sufficiently mobile to form pentagonal islands first that constitute the backbone of the growing layer. On the *i*-Al-Cu-Fe substrate, Pb adatoms appear to be trapped at specific sites before they can diffuse and form islands. Experiments suggest that these sites correspond to cut cluster sites, similar to previous report on Pb adsorption on the fivefold *i*-Al-Pd-Mn quasicrystalline substrate.[12] Because these two substrates are isostructural, the observed differences in the growth of the quasiperiodic monolayer must be a consequence of the different chemistry within the surface termination and the associated change in the surface electronic structure. As mentioned above, the quasicrystalline surface terminations consist of two planes separated by only 0.4 Å, the top plane being almost pure Al and the second one containing a higher content of transition metals.[22] Our results suggest that both planes are important to determine the potential-energy landscape seen by adatoms.

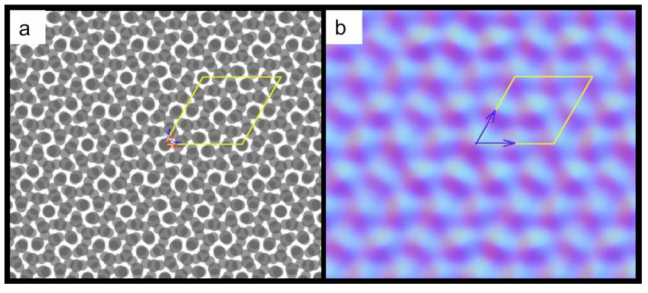

FIG. 9. (Color online) (a) Diagram of the ($\sqrt{31} \times \sqrt{31}$)$R8.95°$ HOC structure using partially transparent circles to represent the atoms. The 15.9 Å unit cell is shown. (b) Smoothed intensity map of the diagram in (a) showing the 15.9 Å unit cell and the 7.95 Å period (arrows).

For both quasicrystalline substrates, the sticking coefficient of Pb drops to zero upon completion of the pseudomorphic monolayer. This is not the case for Pb on Al(111), for which a layer-by-layer growth is observed up to the highest coverages investigated. In addition, the films nucleate at step edges suggesting easy diffusion of Pb adatoms on the Al(111) substrate at room temperature, in contrast to the efficient trapping effect observed on the quasicrystalline substrate. Therefore in one case, the interaction of Pb atoms adsorbed with the quasiperiodic Al-rich plane is highly corrugated, a factor that promotes the 2D pseudomorphic growth.[15,20] On the other side, the interaction between the Pb adsorbate and the fcc Al(111) plane must be flatter in order to promote the formation of the observed moiré structure. Previous studies of Pb on Cu(111) reported 3D island growth upon deposition at room temperature.[42] This 3D growth does not occur on Al(111). The difference relies on the existence of a relative band gap for Cu(111) substrate resulting in electron confinement and quantum size effects affecting the growth in the Pb on Cu(111) system. This is of course not the case for the Al(111) substrate and layer-by-layer growth is observed in agreement with the low surface energy of Pb compared to that of Al.

We have discussed two different possibilities to explain the absence of multilayer growth on quasicrystalline substrates. One is based on the hypothesis that Pb adatoms do stick on the first Pb wetting layer and become extremely mobile and form very large isolated clusters that could not be detected either by STM, LEED, or STM. The other hypothesis is that the sticking coefficient vanishes upon completion of the wetting layer. The sticking probability of an adsorbate on a metal surface depends on the possibility that it loses its kinetic energy. Two main channels for energy dissipation have been proposed, namely, excitations of substrate phonons or formation of electron-hole pairs.[43,44] The electronic structure of the quasiperiodic Pb monolayer formed on *i*-Al-Pd-Mn has been investigated by STS and a deep pseudogap in the electron density of states was found at the Fermi level.[12] The probability for electron-hole pair creation decreases exponentially with increasing binding energy and thus correlates with the density of states at E_F. Therefore the

existence of a pseudogap is consistent with a reduced sticking probability. Nothing is known however about the vibrational density of states of this system and therefore it is impossible to discuss further this issue. We mention however that many other physical properties, such as friction and catalysis, ultimately depend on the mechanism of energy dissipation at the surface. Quasiperiodic Pb monolayers might be useful model systems in this respect.

Finally, the STM and LEED patterns of Pb overlayers on Al(111) are well represented by the $(\sqrt{31}\times\sqrt{31})R8.95°$ HOC structure. As for any HOC structure, the exact structure that forms depends on the balance between adatom-adatom and adatom-substrate interactions. In this case, the Pb-Pb distance remains very close to its natural spacing suggesting that the Pb-Pb interactions dominate the Pb-Al interactions. Although it cannot be ruled out, there is no evidence in this study for a significant reconstruction of the substrate and the presence of the strong 3.48 Å period, close to the natural Pb-Pb distance, suggests little if any intermixing in the monolayer.

ACKNOWLEDGMENTS

We acknowledge the European Network of Excellence on Complex Metallic Alloys (CMA) under Contracts No. NMP3-CT-2005-500145 and No. ANR-05-NT03-41834, and the National Science Foundation under Grant No. DMR-0505160 for financial support.

[1] P. A. Thiel, Annu. Rev. Phys. Chem. **59**, 129 (2008).
[2] V. Fournée and P. A. Thiel, J. Phys. D **38**, R83 (2005).
[3] H. R. Sharma, M. Shimoda, and A. P. Tsai, Adv. Phys. **56**, 403 (2007).
[4] D. Shechtman, I. Blech, D. Gratias, and J. W. Cahn, Phys. Rev. Lett. **53**, 1951 (1984).
[5] A. P. Tsai, Acc. Chem. Res. **36**, 31 (2003).
[6] Z. M. Stadnik, *Physical Properties of Quasicrystals* (Springer, New York, 1999).
[7] T. Cai, J. Ledieu, R. McGrath, V. Fournée, T. Lograsso, A. Ross, and P. Thiel, Surf. Sci. **526**, 115 (2003).
[8] J. Ledieu, J. T. Hoeft, D. E. Reid, J. A. Smerdon, R. D. Diehl, T. A. Lograsso, A. R. Ross, and R. McGrath, Phys. Rev. Lett. **92**, 135507 (2004).
[9] J. Ledieu, J. T. Hoeft, D. E. Reid, J. A. Smerdon, R. D. Diehl, N. Ferralis, T. A. Lograsso, A. R. Ross, and R. McGrath, Phys. Rev. B **72**, 035420 (2005).
[10] J. A. Smerdon, J. Ledieu, J. T. Hoeft, D. E. Reid, L. H. Wearing, R. D. Diehl, T. A. Lograsso, A. R. Ross, and R. McGrath, Philos. Mag. **86**, 841 (2006).
[11] K. J. Franke, H. R. Sharma, W. Theis, P. Gille, P. Ebert, and K. H. Rieder, Phys. Rev. Lett. **89**, 156104 (2002).
[12] J. Ledieu, L. Leung, L. H. Wearing, R. McGrath, T. A. Lograsso, D. Wu, and V. Fournée, Phys. Rev. B **77**, 073409 (2008); J. Ledieu, M. Krajci, J. Hafner, L. Leung, L. H. Wearing, R. McGrath, T. A. Lograsso, D. M. Wu, and V. Fournée, *ibid.* **79**, 165430 (2009).
[13] J. A. Smerdon, L. Leung, J. K. Parle, C. J. Jenks, R. McGrath, V. Fournée, and J. Ledieu, Surf. Sci. **602**, 2496 (2008).
[14] H. R. Sharma, M. Shimoda, A. R. Ross, T. A. Lograsso, and A.-P. Tsai, Philos. Mag. **86**, 807 (2006).
[15] S. Curtarolo, W. Setyawan, N. Ferralis, R. D. Diehl, and M. W. Cole, Phys. Rev. Lett. **95**, 136104 (2005).
[16] V. Fournée, H. R. Sharma, M. Shimoda, A. P. Tsai, B. Unal, A. R. Ross, T. A. Lograsso, and P. A. Thiel, Phys. Rev. Lett. **95**, 155504 (2005).
[17] H. R. Sharma, V. Fournée, M. Shimoda, A. Ross, T. Lograsso, P. Gille, and A. P. Tsai, Phys. Rev. B **78**, 155416 (2008).
[18] J. A. Smerdon, J. K. Parle, L. H. Wearing, T. A. Lograsso, A. R. Ross, and R. McGrath, Phys. Rev. B **78**, 075407 (2008).
[19] M. Krajci and J. Hafner, Phys. Rev. B **71**, 184207 (2005).
[20] W. Setyawan, R. D. Diehl, N. Ferralis, M. W. Cole, and S. Curtarolo, J. Phys.: Condens. Matter **19**, 016007 (2007).
[21] B. Bilki, M. Erbudak, M. Mungan, and Y. Weisskopf, Phys. Rev. B **75**, 045437 (2007).
[22] T. Cai, F. Shi, Z. Shen, M. Gierer, A. I. Goldman, M. J. Kramer, C. J. Jenks, T. A. Lograsso, D. W. Delaney, P. A. Thiel, and M. A. Van Hove, Surf. Sci. **495**, 19 (2001).
[23] T. Cai, V. Fournée, T. A. Lograsso, A. R. Ross, and P. A. Thiel, Phys. Rev. B **65**, 140202(R) (2002).
[24] H. R. Sharma, V. Fournée, M. Shimoda, A. R. Ross, T. A. Lograsso, A. P. Tsai, and A. Yamamoto, Phys. Rev. Lett. **93**, 165502 (2004).
[25] Z. Papadopolos, G. Kasner, J. Ledieu, E. J. Cox, N. V. Richardson, Q. Chen, R. D. Diehl, T. A. Lograsso, A. R. Ross, and R. McGrath, Phys. Rev. B **66**, 184207 (2002).
[26] B. Unal, C. J. Jenks, and P. A. Thiel, Phys. Rev. B **77**, 195419 (2008).
[27] D. Gratias, F. Puyraimond, M. Quiquandon, and A. Katz, Phys. Rev. B **63**, 024202 (2000).
[28] J. Ledieu, P. Unsworth, T. Lograsso, A. Ross, and R. McGrath, Phys. Rev. B **73**, 012204 (2006).
[29] J. A. Smerdon, H. R. Sharma, J. Ledieu, and R. McGrath, J. Phys.: Condens. Matter **20**, 314005 (2008).
[30] C. Ghosh, D. J. Liu, C. J. Jenks, P. A. Thiel, and J. W. Evans, Philos. Mag. **86**, 831 (2006).
[31] C. Ghosh, D. J. Liu, K. J. Schnitzenbaumer, C. J. Jenks, P. A. Thiel, and J. W. Evans, Surf. Sci. **600**, 2220 (2006).
[32] M. Krajčí and J. Hafner, Phys. Rev. B **77**, 134202 (2008).
[33] L. Floreano, D. Cvetko, F. Bruno, G. Bavdek, A. Cossaro, R. Gotter, A. Verdini, and A. Morgante, Prog. Surf. Sci. **72**, 135 (2003).
[34] U. Dahmen, S. Q. Xiao, S. Paciornik, E. Johnson, and A. Johansen, Phys. Rev. Lett. **78**, 471 (1997).
[35] A. Landa, P. Wynblatt, E. Johnson, and U. Dahmen, Acta Mater. **48**, 2557 (2000).
[36] T. Wiederholt, H. Brune, J. Wintterlin, R. J. Behm, and G. Ertl, Surf. Sci. **324**, 91 (1995).
[37] C. R. Ast, Daniela Pacilé, Marco Papagno, Thomas Gloor, Frédéric Mila, Stephan Fedrigo, Gero Wittich, Klaus Kern, Harald Brune, and Marco Grioni, Phys. Rev. B **73**, 245428 (2006).

[38] M. Morscher, M. Corso, T. Greber, and J. Osterwalder, Surf. Sci. **600**, 3280 (2006).
[39] K. J. Rawlings, M. J. Gibson, and P. J. Dobson, J. Phys. D **11**, 2059 (1978).
[40] L. Vitos, A. V. Ruban, H. L. Skriver, and J. Kollar, Surf. Sci. **411**, 186 (1998).
[41] A. Tkatchenko, Phys. Rev. B **75**, 235411 (2007).
[42] R. Otero, A. Vasquez de Parga, and R. Miranda, Phys. Rev. B **66**, 115401 (2002).
[43] K. Schönhammer and O. Gunnarsson, Phys. Rev. B **22**, 1629 (1980).
[44] K. Schönhammer and O. Gunnarsson, Phys. Rev. B **24**, 7084 (1981).